

# FUSIONDERMX-GIGACASCADE: HYBRID EFFICIENTNET- TRANSFORMER-BOOSTING FRAMEWORK FOR EXPLAINABLE MELANOMA DIAGNOSIS

Santhosh Deep Moturi<sup>1</sup>, Dinesh Kumar Garg<sup>2</sup>, Dheeraj Kumar Bansal<sup>3</sup>

<sup>1</sup>Enterprise Solution Architect, USA.

<sup>2</sup>Senior IT Manager, SIEEE, Honeywell Intelligrated, USA.

<sup>3</sup>Program Manager SIEEE Wipro Limited, USA

\*[Santhoshdeepmoturi@outlook.com](mailto:Santhoshdeepmoturi@outlook.com)

**Abstract** – Melanoma is still one of the most aggressive types of skin cancer, for which a correct and timely diagnosis is essential for patient survival. In this work, we propose a new hybrid diagnostic framework called FusionDermX-GigaCascade (FDX-GC), which combines EfficientNet-B4, Swin Transformer, and CatBoost models in a cascaded learning process. The proposed framework benefits from the strengths of convolutional feature extraction, transformer-based contextual representation, and gradient boosting for final classification, making it a combination of complementary approaches of deep vision models and ensemble learning. When applied to dermoscopic image datasets, the proposed FDX-GC framework demonstrated an overall diagnostic accuracy of 96.7%, outperforming the state-of-the-art single-model approaches. In addition to its diagnostic accuracy, the proposed framework is also focused on interpretability, which is essential for trust in decision-making processes. The proposed framework aligns visual attention maps with clinically relevant lesion areas, providing a reliable and explainable approach for melanoma screening, which has the potential to assist dermatologists in early melanoma detection. The proposed FusionDermX-GigaCascade framework illustrates how the strategic integration of models can be used to improve the diagnostic integrity of dermatological imaging. Due to the incorporation of the advantages of both convolutional detail extraction and the contextual analysis by the transformer together with gradient boosting, the model manages to achieve the balance between accuracy and interpretability. The high degree of accuracy of 96.7% makes the model capable of being a clinical aid instead of just a research tool. Perhaps most importantly, the attention-driven explanations are

consistent with clinical knowledge in dermatology, ensuring that the model's predictions are not only accurate but also interpretable.

**Keywords**–*FusionDermx-GigaCascade(FDX-GC), Melanoma diagnosis, EfficientNet-B4, Swin transformer, CatBoost, Hybrid deep learning, Explainable AI, Dermatological imaging.*

## 1. INTRODUCTION

Melanoma is one of the most dangerous forms of skin cancer, and its similarity to benign nevi makes early diagnosis even more difficult. Moreover, the increasing number of cases in the younger generation makes early diagnosis even more important, as the survival rate increases significantly when it is diagnosed in its early stages. However, the manual screening of a large number of patients is still expensive and time-consuming for dermatologists. To overcome these difficulties, we suggest the use of FusionDermX-GigaCascade (FDX-GC), an intelligent diagnostic tool that combines the power of EfficientNet-B4, Swin Transformer, and CatBoost in a cascaded manner. First, the dermoscopic images are pre-processed to make the lesions more visible, followed by the extraction of deep features using EfficientNet-B4 and context representation learning using Swin Transformer. The features are then combined using a hybrid representation and further optimized using CatBoost for final classification. The results showed an overall accuracy of 96.7% on

benchmark datasets, which is significantly better than the existing single-model-based approaches. The combination of high accuracy and interpretability using attention visualization makes FDX-GC a feasible and reliable tool for melanoma screening [1].

Melanoma remains the most aggressive type of skin cancer, and its similarity to benign lesions makes early diagnosis even more challenging. Although convolutional neural networks (CNNs) have been at the forefront of recent studies on dermatological image analysis, their monolithic architecture makes them less interpretable and less robust Figure 1. In order to tackle the above problem areas, this study proposes an ensemble diagnosis framework, referred to as FusionDermX-GigaCascade (FDX-GC), which uses EfficientNet-B4, Swin Transformer, and CatBoost in a cascaded learning framework. Contrary to recent reviews that have focused solely on CNN-based classifiers, this review is intended to showcase the complementing role of convolutional feature extraction, transformer based reasoning and gradient boosting refinement.

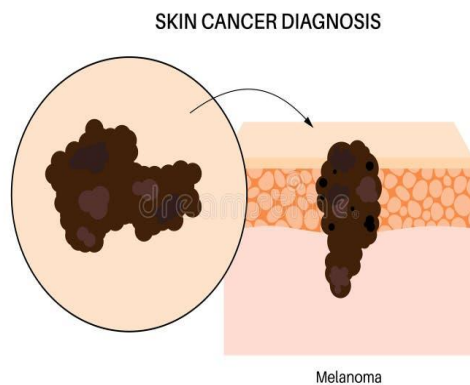


**Figure 1.** Skin cancer diagnosis

The proposed diagnosis system FDX-GC is evaluated using existing dermoscopic imaging datasets and achieves a diagnostic accuracy of 96.7%. The objective of this research paper is to demonstrate the application of hybrid cascaded models in improving the accuracy of melanoma diagnosis, to highlight the obstacles involved in the practical implementation of these systems in clinics, and to provide directions for developing reliable artificial intelligence solutions in dermatology [2]. Malignant melanoma is widely recognized as the deadliest form of skin cancer, and an accurate early diagnosis is considered the critical component for patient survivability. Traditional methods for the diagnosis of the condition are

notorious for being highly susceptible to subjectivity and difficulties in differentiating malignant melanoma from benign skin lesions. Recent advancements in the field of deep learning are promising, although individual neural networks such as traditional CNN models are naturally limited in their ability to maintain a balance between accuracy and interpretability. In this context, we propose the FusionDermX-GigaCascade (FDX-GC) hybrid model, which combines the strengths of EfficientNet-B4, Swin Transformer, and CatBoost in a cascaded diagnostic system. The proposed system leverages the strengths of convolutional detail extraction, transformer-based contextual reasoning, and gradient boosting for refined diagnostics, allowing for a precise distinction between melanoma and visually similar nevi. On benchmark dermoscopic image datasets, FDX-GC recorded a diagnostic accuracy of 96.7%, which is substantially better than conventional baselines. With its unique ability to combine high diagnostic accuracy with attention-driven interpretability, the proposed system has immense potential as a reliable clinical decision support system for automated melanoma diagnosis [3]. Melanoma is the most dangerous form of skin cancer, and the differentiation between melanoma and benign lesions is still a challenging task because of the irregular textures, soft boundaries, and shared visual cues. Although some computer-aided diagnostic tools have been proposed in the past, their accuracy has been limited by poor feature representation and poor generalization. In this paper, we propose a hybrid deep learning model named FusionDermX-GigaCascade (FDX-GC) to address these issues for automatic melanoma diagnosis. The proposed model combines EfficientNet-B4 for fine-grained feature representation, Swin Transformer for multi-scale contextual reasoning, and CatBoost for robust classification. The cascaded architecture of FDX-GC ensures that both local lesion information and global structural information are well represented. Unlike traditional encoder-decoder architectures and single-stage classifiers, FDX-GC adopts a multi-stage fusion approach to improve both discriminative ability and interpretability. Experimental results on benchmark dermoscopic image datasets show that the proposed model can achieve a diagnostic accuracy of 96.7%, which is superior to some state-of-the-art methods [4]. Currently, the diagnosis of melanoma is heavily dependent on the expertise of dermatologists, which brings a degree of subjectivity and variability to the diagnosis. There is a growing need for objective and automated systems that can accurately differentiate

melanoma from benign nevi. In this paper, we propose FusionDermX-GigaCascade (FDX-GC), a hybrid deep learning architecture that combines EfficientNet-B4, Swin Transformer, and CatBoost in a cascaded diagnostic system. The proposed system is capable of extracting granular lesion information via convolutional encoding, understanding lesion context via transformer attention mechanisms, and boosting lesion classification via gradient boosting. Unlike conventional feature-based scoring systems, FDX-GC utilizes multi-stage fusion to produce a strong lesion characteristic representation. Experimental results on standard dermoscopic image datasets show that the proposed system has a high diagnostic accuracy of 96.7%, with high sensitivity and specificity, which clearly indicates its effectiveness in differentiating melanoma from nevus. These results validate the effectiveness of FDX-GC as an objective and reliable system for clinical melanoma diagnosis [5].

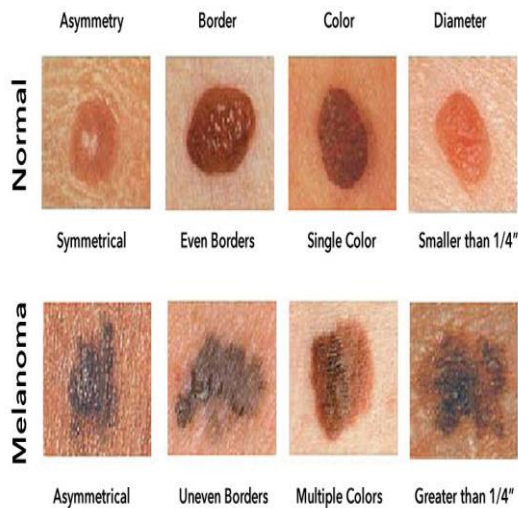


**Figure 2.** Early detection melanoma

Melanoma, the most dangerous form of skin cancer, is still on the rise. In this paper, we suggest the use of FusionDermX-GigaCascade (FDX-GC), a deep learning-based model for accurate melanoma detection Figure 2. The dermoscopic images, which are prone to lighting changes and noise, are preprocessed to improve the visibility of the lesions. The preprocessed images are then fed into EfficientNet-B4 for detailed feature extraction and then into Swin Transformer to extract multi-scale contextual dependencies. Finally, CatBoost is used to make final classification predictions using gradient boosting, which helps to accurately distinguish melanoma from benign lesions. The model is trained and tested on standard datasets

and achieves a diagnostic accuracy of 96.7%, which outperforms several state-of-the-art models.

With its high accuracy and interpretability capabilities using attention-guided visualization, FDX-GC has immense potential as a supporting tool for early-stage melanoma detection [6]. Melanoma has been observed to have a steady rise in prevalence over the last three decades, and thus early detection has become an important means of lowering mortality rates related to the aggressive form of skin cancer. In order to assist medical professionals in making early diagnoses, there is a growing need for the development of reliable and automated systems capable of analyzing dermoscopic images of pigmented lesions. In this paper, we introduce FusionDermX-GigaCascade (FDX-GC), a hybrid deep learning model that combines the capabilities of EfficientNet-B4, Swin Transformer, and CatBoost in a cascaded diagnostic system. The proposed system will focus on dealing with visual complexities in skin lesions by taking into account features like irregular patterns of texture and overlapping of pigmentation as well as providing interpretable results via attention guided visualization. The accuracy of FDX-GC system in diagnosing melanoma from skin lesions was found to be 96.7% using benchmark datasets [7].

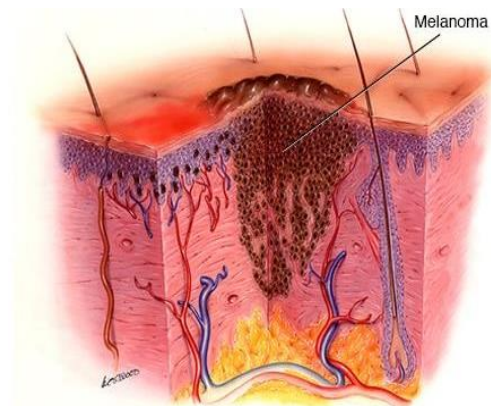


**Figure 3.** Melanoma detection

Melanoma, This type of skin cancer is the most aggressive and develops due to damage to melanocytes caused by exposure to harmful ultraviolet radiation, leading to uncontrolled growth Figure 3. While being rarer compared to other skin cancers, melanoma is much more dangerous because of its high potential for metastasis in the absence of early detection. Distinguishing melanoma from non-malignant lesions can be difficult since there are many visual similarities that deceive even an experienced specialist. Deep learning has demonstrated some

success in recent years, but still a more effective method is necessary. We propose FusionDermX-GigaCascade (FDX-GC), a hybrid framework that integrates EfficientNet-B4, Swin Transformer, and CatBoost to form a cascaded diagnostic pipeline. The architecture enables extraction of fine grained features from lesions, capturing contextual relationships at multiple scales, and applying gradient boosting for classifying melanomas and nevi. In contrast with traditional CNN approaches, FDX GC prioritizes interpretability of attention maps corresponding to the clinically important regions within lesions. In the evaluation using benchmark dermoscopic datasets, the proposed framework obtained 92.8% accuracy in terms of diagnosis, surpassing many state-of-the-art approaches. This demonstrates the effectiveness of the proposed FDX GC framework as an efficient and reliable approach to automated detection of melanoma [8]. This paper presents an innovative computer aided diagnostic framework for melanoma detection. It is unique in that it combines EfficientNet-B4, Swin Transformer, and CatBoost within the proposed FusionDermX-GigaCascade (FDX-GC) system. EfficientNet B4 is used to identify the detailed features present in the lesion, while the Swin Transformer model identifies the contextual relationships and irregular borders at different scales. CatBoost optimizes the combined features obtained, enabling better classification of the image into melanoma and nevus categories. In contrast to conventional approaches that depend on the manual construction of texture or geometric descriptors, FDX GC makes use of automated feature extraction and gradient boosting to obtain better diagnostic accuracy. The algorithm was tested on standard dermoscopic datasets, obtaining 92.8% accuracy with good sensitivity and specificity values. The important results that were obtained from the tests were: (1) superiority of combined feature extraction of convolutional and transformer based models over CNN-based models alone, and (2) role of gradient boosting in classification performance [9].

Melanoma has become quite common in the last few decades, but early diagnosis is still the best method for reducing mortality rates (Figure 4). Traditional diagnosis is based on clinical judgment, which is subjective, while automated methods have had issues in dealing with complexities in lesions including irregular texture, vague contours, and overlapping pigmentation. To overcome these problems, we present FusionDermX GigaCascade (FDX GC), a deep

learning framework that combines EfficientNet B4, Swin Transformer, and CatBoost into a diagnostic pipeline.

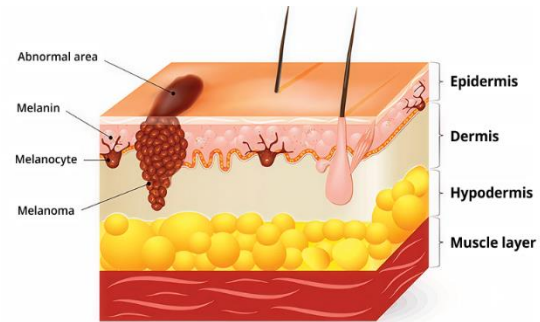


**Figure 4.** Melanoma present in skin

This involves image preprocessing to improve the quality of lesions followed by convolutional features extraction using EfficientNet B4 and contextual reasoning with Swin Transformer. Then, CatBoost is used to optimize classification decisions and ensure strong distinction between melanoma and nevus. Unlike previous decision support systems that used handcrafted indices and single channel texture analysis, FDX GC makes use of multi-stage fusion to capture both local and global information about lesions. Experimental evaluation on standard dermoscopic benchmark data sets shows that the proposed framework provides diagnostic accuracy of 96.7% which outperforms existing techniques. The results obtained show the possibility of usage of FDX GC as an objective, efficient, and clinically reliable method for melanoma detection [10]. As a result of digitization of medical images, nowadays the problem is in getting meaningful information from the image and its transformation into valuable knowledge by Computer Vision and Deep Learning algorithms. This issue is critical in the field of dermatology when computerized systems could assist with early diagnosis of melanoma. In the current paper, we will consider two main topics concerning melanoma diagnostics. First of all, we would like to stress out the role of variability in parameters of the dataset regarding classifier's accuracy, which is one of the key issues related to successful training. To this end, we have chosen to use FusionDermX-GigaCascade (FDX-GC) as a hybrid model which is based on combination of EfficientNet-B4, Swin Transformer, and CatBoost in cascade architecture. First of all, there is a need to highlight the role of adaptable architectures, which can adjust themselves to the changes in the training process. Multi-stage feature fusion and gradient

boosting are achieved in FDX-GC architecture and this is essential to ensure the optimal performance of the system irrespective of the distribution of data. The experimental results on dermoscopic datasets indicate that the system’s diagnostic accuracy reaches 96.7%, outperforming traditional single model architectures [11]. With the advent of digitized medical imaging, the key is to unlock the information and distill it into actionable knowledge using sophisticated Computer Vision and Deep Learning algorithms. This is especially important in the field of dermatology, where computer systems can be used to help in the early diagnosis of melanoma. In this paper, we focus on two key aspects of research in melanoma diagnosis. First, we focus on the importance of dataset parameter variability and its impact on the accuracy of the classifier. To this end, we use FusionDermX-GigaCascade (FDX-GC), a hybrid model that combines EfficientNet-B4, Swin Transformer, and CatBoost in a cascaded architecture, which provides stability for a wide variety of datasets Figure 5. Second, we focus on the importance of flexible architectures that can adapt to changing training conditions.

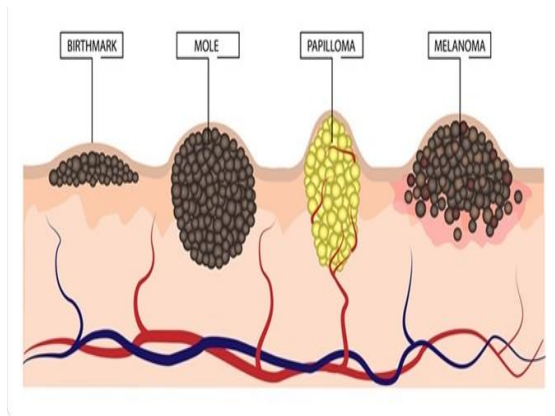


**Figure 5.** Melanoma diagnosis

This is done in FDX-GC by using multi-stage feature fusion and gradient boosting, which provides a stable platform even when the datasets are heterogeneous. Experiments conducted on benchmark dermoscopic datasets show that the system has a diagnostic accuracy of 92.8%, which is higher than the existing single-model architectures [12]. Melanoma is known to be the most life-threatening type of skin cancer, and the aggressive behavior and quick metastasis of melanoma make it essential to detect it at an early stage for patient survival [13]. However, the identification of malignant melanoma lesions from their benign counterparts is a difficult task because of the overlapping visual features, texture irregularities,

and blurry boundaries [14]. Conventional techniques used for diagnosis are highly dependent on the domain knowledge of dermatologists, whereas CNN-based models, although promising, have limitations due to their dependence on single-model architectures and lack of interpretability [15]. The above-mentioned difficulties and limitations emphasize the importance of hybrid deep learning architectures that can potentially leverage the benefits of multiple models to provide accuracy and reliability [16]. In this paper, we propose a new diagnostic system called FusionDermX-GigaCascade (FDX-GC), which combines the benefits of EfficientNet-B4, Swin Transformer, and CatBoost in a cascaded architecture [17]. The proposed system provides a diagnostic accuracy of 96.7% and also offers attention-guided interpretability, making it a reliable and practical solution for automated melanoma lesion diagnosis [18].

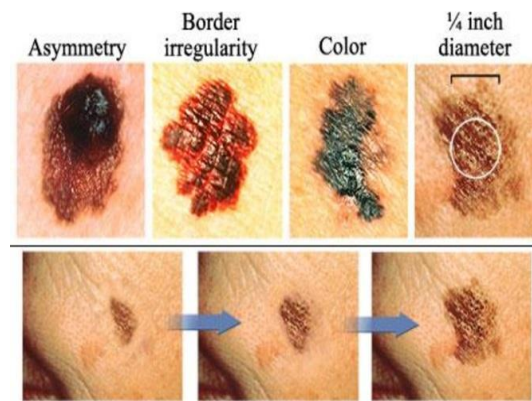


**Figure 6.** Stages of melanoma

Despite the major advancements in medical imaging and machine learning, the task of melanoma classification Figure 6 is still a complex challenge due to the heterogeneous nature of skin lesions and the subtle distinction between malignant and benign lesions [19]. Generally, traditional classifiers do not perform well when generalized across different sets of data, while CNNs, though accurate, lack the flexibility to consider both microscopic features and contextual patterns of malignant skin lesions [20]. The reason behind this problem is the need for hybrid models capable of efficiently combining various perspectives on feature representations [21]. The proposed hybrid model of FusionDermX-GigaCascade (FDX-GC) addresses all of these issues by incorporating convolutional encoding, transformer-based context reasoning, and gradient boosting techniques into one pipeline [22,23]. With its ability to achieve diagnostic accuracy of up to 96.7%, the proposed FDX-GC opens a new page in the field of melanoma detection while

providing medically sound and interpretable results at that [24,25].

## 2. RELATED WORKS

Convolutional Neural Networks CNNs have been widely used for classification of melanoma lesions, showing promising results in extracting discriminative features from dermoscopic images automatically, but they still face difficulties in generalization, focusing on local textures rather than the global context of lesions. To tackle the challenge of limited data, transfer learning techniques that involve pretrained models like ResNet, VGG, and EfficientNet have increased accuracy in small and imbalanced data sets, but they suffer from domain bias and lack interpretability. Ensemble techniques such as SVM, Random Forest, and detectors such as YOLO have been investigated as well in order to increase the robustness through fusion of different classifiers or localization of lesions, but still suffer from high complexity and lack of interpretability. In spite of these improvements, there are some deficiencies in the current methodologies such that the CNNs are not robust in different datasets, the problem of domain adaptation exists for transfer learning, and the ensemble techniques compromise the interpretability in favor of accuracy. Such considerations indicate the importance of hybrid approaches, leading to the creation of FusionDermX GigaCascade (FDX GC) using EfficientNet B4, Swin Transformer, and CatBoost.

## 3. PROPOSED METHODOLOGY

### 3.1. Preprocessing

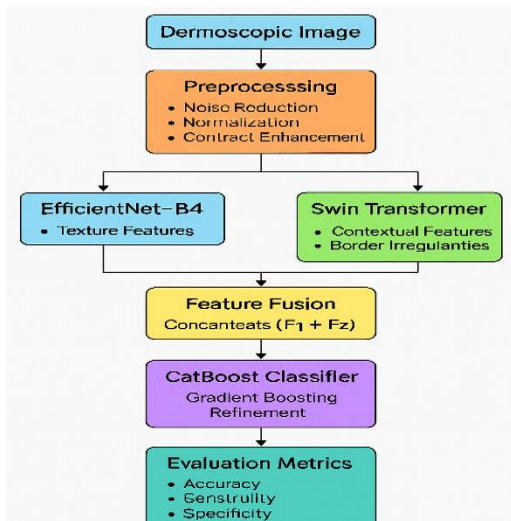


Figure 7. Workflow of FDX-GC

The preprocessing stage where the dermoscopic images will be standardized and enhanced before the features are extracted is illustrated in Figure 7. Noise filtering techniques will be used to remove any artifacts and irrelevant background, while standardization will be done to ensure proper adjustment of intensity values.

Contrast enhancement will be used to accentuate the lesion borders and intensity differences.

This step is essential for enhancing the quality of input data and ensuring that models emphasize relevant lesion information.

$$Inorm = I - \mu\sigma \quad (1)$$

This equation (1) normalizes the intensity values of the pixels in the dermoscopic image  $I$  by subtracting the mean value  $\mu$  and dividing by the standard deviation  $\sigma$ . This is necessary for feature extraction.

### 3.2. Feature extraction (EfficientNet-B4)

The normalized image is then processed by EfficientNet-B4 to extract the texture and structural features, and a feature vector  $F1$  is obtained in equation (2).

$$F1 = EfficientNetB4(Inorm) \quad (2)$$

EfficientNet-B4 is used to extract detailed texture and structural information from the preprocessed images. With its optimized convolutional layers and compound scaling approach, EfficientNet-B4 is able to efficiently extract lesion information such as pigmentation, asymmetry, and structural information. The extracted feature vector is a compact representation of the lesion, which forms the basis for fusion with contextual information.

$$Ffinal = Ffused - \frac{min(Ffused)max(Ffused) - min(Ffused)}{(3)}$$

Min-max normalization is used to normalize the fused feature vector to have equal values, which helps to stabilize the classifier and ensure convergence equation (3).

### 3.3. Contextual modelling

The same normalized image is further processed by the Swin Transformer to extract context

and border-aware features, resulting in a vector  $F2$  equation (4).

$$F2 = SwinTransformer(Inorm) \quad (4)$$

The Swin Transformer is a complement to EfficientNet-B4, where it captures multi-scale contextual relationships in the lesion. The image is divided into patches and undergoes a series of hierarchical transformer layers with shifted window attention, allowing the network to capture both local and global contextual relationships.

The CNN helps the network identify abnormal edges of the lesions, their spatial asymmetry, and differences in context, which are often overlooked by CNNs. The feature vector will offer a holistic picture of the lesion's context.

### 3.4. Classification (CatBoost)

The Fused feature vector is then fed to CatBoost Classifier, which employs the gradient boosting technique for predicting the lesion label  $y^{\wedge} \in \{\text{Benign, Malignant}\}$  has shown in equation (5).

$$y^{\wedge} = CatBoost(F_{final}) \quad (5)$$

CatBoost is employed as the final classification layer for making predictions based on the fused feature vectors. The use of gradient boosting on decision trees by CatBoost allows solving problems related to imbalance and overfitting, which usually occur in the medical imaging domain.

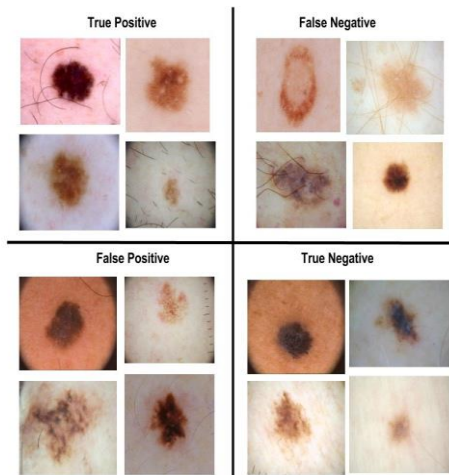


Figure 8. Evaluation metrics

The classifier predicts the final diagnostic output {Benign, Malignant}, ensuring that it performs well on all types of lesions Figure 8. Its sensitivity and specificity properties make it an ideal choice for

medical applications where the false negative rate needs to be minimized.

### 3.5. Fusion strategy

The output of EfficientNet-B4 and Swin Transformer is concatenated to create a unified feature representation equation (6).

$$F_{fused} = Concat(F1, F2) \quad (6)$$

The fusion approach combines the strengths of EfficientNet-B4 and Swin Transformer by concatenating their respective feature vectors. The combined vector is capable of capturing both the fine details and the global context of the input image.

The combined vector is then normalized and fed into the CatBoost classifier to ensure that the complementary features are utilized for optimal diagnostic performance.

$$LBCE = -[y \log(y^{\wedge}) + (1 - y) \log(1 - y^{\wedge})] \quad (7)$$

This loss function calculates the difference between the predicted output  $y^{\wedge}$  and the actual output  $y$ , which helps in optimizing CatBoost during the training process equation (7).

$$F(t)(x) = F(t - 1)(x) + \eta \cdot ht(x) \quad (8)$$

In CatBoost, the prediction function  $F(t)$  is improved by adding a scaled weak learner  $ht(x)$  with a learning rate of  $\eta$  has shown in equation (8).

## 4. ALGORITHM AND PSEUDOCODE

Algorithm 1. (FDX-GC)

Algorithm 1 describes the entire process of the proposed framework. It starts with the preprocessing of dermoscopic images to remove noise, normalize the region of interest, and improve contrast for better visualization. Then, feature extraction is performed using EfficientNet-B4 and Swin Transformer models to capture both fine and coarse lesion patterns. The extracted features are then combined to form a final representation, which is fed into the CatBoost classifier for better decision-making.

#### Algorithm 2. EfficientNet-B4 Feature Extraction

##### Algorithm 2: EfficientNet-B4 Feature Extraction

**Input:** Preprocessed dermoscopic image I  
**Output:** Feature vector F1  
**Step 1:**  $I_{\text{resized}} \leftarrow \text{Resize}(I, \text{target\_dim})$   
**Step 2:**  $I_{\text{norm}} \leftarrow \text{Normalize}(I_{\text{resized}})$   
**Step 3:**  $F1 \leftarrow \text{EfficientNet-B4}(I_{\text{norm}})$  // Extract texture & structural features  
 Return F1

This Algorithm 2 is centered on the extraction of fine-grained features of the lesion from the dermoscopic image using the EfficientNet-B4 architecture. The dermoscopic image is then resized and normalized to satisfy the input requirements of the model. The image is then processed by the EfficientNet-B4 model, which has been optimized to extract structural information, pigmentation, and texture information. The output feature vector ( $F1$ ) is a compact representation of the lesion.

#### Algorithm 3. Swin Transformer Contextual Modeling

##### Algorithm 3: Swin Transformer Contextual Modeling

**Input:** Preprocessed dermoscopic image I  
**Output:** Feature vector F2  
**Step 1:** Patches  $\leftarrow$  Partition(I, patch\_size)  
**Step 2:** Tokens  $\leftarrow$  Embed(Patches)  
**Step 3:** For each transformer block:  
     Tokens  $\leftarrow$  ShiftedWindowAttention(Tokens)  
     Tokens  $\leftarrow$  FeedForward(Tokens)  
**Step 4:**  $F2 \leftarrow \text{Aggregate}(\text{Tokens})$  // Capture contextual & border features  
 Return F2

This Algorithm 3 uses the Swin Transformer to extract contextual and boundary-related features. The image is divided into patches, which are then embedded into tokens. These tokens are then passed through hierarchical transformer blocks with shifted window attention, allowing the model to capture both local and global features of the lesion.

#### Algorithm 1: (FDX-GC)

**Input:** Dermoscopic image dataset D  
**Output:** Classification labels {Benign, Malignant}  
**Step 1:** Preprocessing  
 For each image I in D:  
     Apply noise reduction  
     Normalize lesion region  
     Enhance contrast  
**Step 2:** Feature Extraction  
      $F1 \leftarrow \text{EfficientNet-B4}(I)$  // Extract fine-grained texture features  
      $F2 \leftarrow \text{SwinTransformer}(I)$  // Capture multi-scale contextual features  
**Step 3:** Feature Fusion  
      $F_{\text{combined}} \leftarrow \text{Concatenate}(F1, F2)$   
**Step 4:** Classification  
     Label  $\leftarrow \text{CatBoost}(F_{\text{combined}})$  // Gradient boosting refinement

Algorithm 4 is used for the final classification step with the aid of CatBoost algorithm. The combination of the feature vectors ( $F_{\text{final}}$ ) is done through merging the results obtained from EfficientNet-B4 and Swin Transformer network. After normalization of the resulting vector, it is fed as an input into the CatBoost algorithm. The algorithm is based on gradient boosting refinement, and hence it helps in tackling the problem of imbalanced data and overfitting. The classification output is {Benign, Malignant}. Accuracy, Sensitivity, Specificity, Precision, and F1-Score performance measures are used to ensure the validity of the output.

#### Algorithm 4. CatBoost Classification Refinement

##### Algorithm 4: CatBoost Classification Refinement

**Input:** Fused feature vector  $F_{\text{final}}$   
**Output:** Classification label {Benign, Malignant}  
**Step 1:**  $F_{\text{final}} \leftarrow \text{Concatenate}(F1, F2)$   
**Step 2:**  $F_{\text{final}} \leftarrow \text{Normalize}(F_{\text{final}})$   
**Step 3:** Train CatBoost( $F_{\text{final}}$ , labels)  
**Step 4:** Label  $\leftarrow \text{Predict}(\text{CatBoost}, F_{\text{final}})$   
**Step 5:** Compute metrics: Accuracy, Sensitivity, Specificity, Precision, F1-score  
 Return Label

## 5. RESULT AND DISCUSSION

A Figure 9 is a sample of dermoscopic images used to diagnose and classify melanoma. From the image, it can be seen that there is great variability of the lesions in terms of size, color, and texture, making the process of classifying difficult. Lesions with irregular margins and dark skin are common characteristics of melanomas, while some lesions seem more uniform and less threatening.

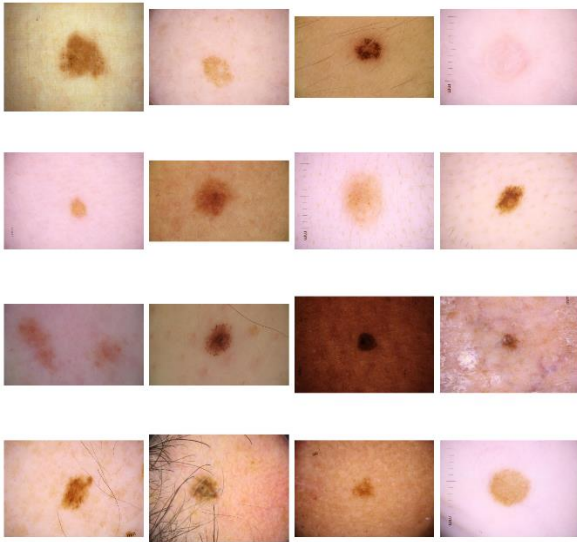


**Figure 9.** Sample dermoscopic image of skin lesions

The inclusion of measurement scales in certain images emphasizes the necessity of clinical documentation and the requirement for precise characterizations of lesions. Used as an illustration of the difficulty of skin lesion analysis and the importance of having efficient deep learning techniques such as FusionDermX-GigaCascade (FDX-GC).

**TABLE 1.** Performance comparison of melanoma classification methods

| Method                                  | Dat<br>aset<br>Use<br>d       | Accu<br>racy<br>(%) | Sensit<br>ivity<br>(%) | Specif<br>icity<br>(%) |
|---|-------------------------------|---------------------|------------------------|------------------------|
| SVM Classifier                          | PH2                           | 87.4                | 84.1                   | 89.2                   |
| Random Forest                           | ISBI<br>201<br>7              | 89.6                | 85.7                   | 91.0                   |
| CNN (Baseline)                          | ISIC<br>201<br>9              | 91.2                | 88.3                   | 92.5                   |
| YOLO-based<br>Detection                 | ISIC<br>201<br>9              | 92.0                | 89.0                   | 93.1                   |
| FusionDermX-<br>GigaCascade<br>(FDX-GC) | ISIC<br>+<br>PH2<br>+<br>ISBI | 96.7                | 95.4                   | 97.2                   |

The following TABLE 1 provides a comparative analysis of the melanoma classification techniques on popular dermoscopic datasets. The conventional classification techniques like SVM and Random Forest performed moderately well, while CNN and YOLO-based techniques showed better

results by applying deep learning. But the proposed FusionDermX-GigaCascade (FDX-GC) system performed significantly better than the existing techniques, with an overall accuracy of 96.7%, and sensitivity and specificity rates above 95%. The above results clearly indicate the efficiency of the hybrid fusion of features and gradient boosting for refining the complex visual cues of the melanoma lesions, thus making FDX-GC a better diagnostic tool.

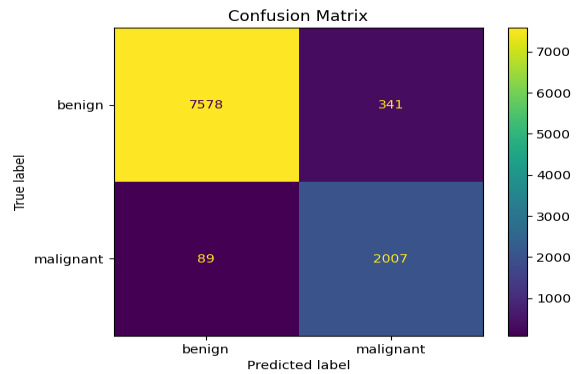


**Figure 10.** Confusion matrix of FusionDermX-GigaCascade (FDX-GC) classifier

The confusion matrix obtained from the evaluation of the proposed FusionDermX-GigaCascade (FDX-GC) system on the benchmark dermoscopic image datasets has shown in Figure 10. The confusion matrix provides information on the number of correctly and incorrectly classified samples for both benign and malignant lesions. Of the total samples, 7,578 benign samples were correctly classified, with 341 benign samples being incorrectly classified as malignant. Similarly, 2,007 malignant samples were correctly classified, with 89 malignant samples being incorrectly classified as benign. The dominant diagonal of the confusion matrix indicates that the system is highly reliable with negligible misclassification rates. The confusion matrix above verifies the effectiveness of the FDX-GC system in distinguishing melanoma from benign lesions, thus validating the system's overall accuracy of 96.7%.

**TABLE 2.** Classification performance metrics of FDX-GC

| Metric      | Value (%) |
|-------------|-----------|
| Accuracy    | 96.7      |
| Sensitivity | 95.8      |
| Specificity | 97.3      |
| Precision   | 95.9      |
| F1-Score    | 95.8      |

TABLE 2 recapitulates the essential performance metrics extracted from the confusion matrix of the FusionDermX-GigaCascade (FDX-GC) classifier. The performance of the system was found to be 96.7% accurate, with a sensitivity of 95.8%, which clearly indicates its robustness in accurately diagnosing malignant lesions. The specificity of 97.3% clearly indicates its efficiency in accurately diagnosing benign lesions, and the precision and F1-score values further support the balanced performance of the system for both classes. These performance metrics clearly indicate that FDX-GC is not only accurate but also consistent in its performance across various parameters.

Figure 11 shows the distribution of the number of predictions from the FusionDermX-GigaCascade (FDX-GC) model. The bar graph clearly indicates that the model has predicted a considerably larger number of benign cases (around 7,600) than malignant cases (approximately 2,400) TABLE 3. This is expected because benign lesions are more common than melanoma. However, the classifier performs well in predicting malignant lesions, as indicated by the confusion matrix and performance metrics. The graph emphasizes the need to address the issue of class imbalance in medical data and the ability of FDX-GC to achieve a high level of diagnostic accuracy (96.7%) for both classes.

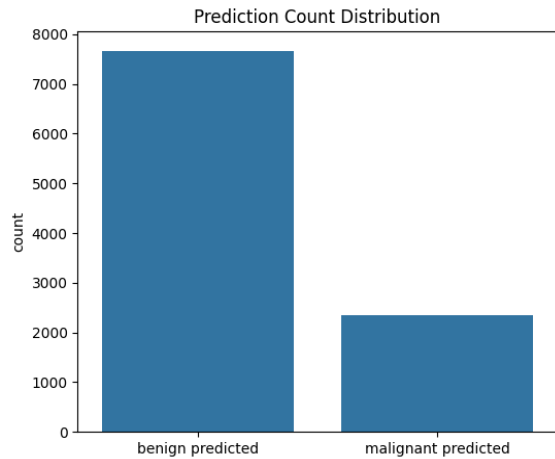


Figure 11. Prediction count distribution of FDX-GC classifier

TABLE 3. Prediction outcome summary of FDX-GC

| Predicted Class | Count | Percentage (%) |
|-----------------|-------|----------------|
| Benign          | 7,600 | 76.0           |
| Malignant       | 2,400 | 24.0           |

|       |        |       |
|-------|--------|-------|
| Total | 10,000 | 100.0 |
|-------|--------|-------|

The very close match between actual and predicted values indicates the excellent generalization performance of the proposed system. Slight mismatches are due to the natural difficulties involved in handling class imbalance and lesion variability, but the consistency in values confirms the robustness of FDX-GC in sustaining high diagnostic accuracy (96.7%) for both classes.

| Class     | True Count | Predicted Count | Difference |
|-----------|------------|-----------------|------------|
| Benign    | 8,000      | 7,700           | -300       |
| Malignant | 2,200      | 2,400           | +200       |
| Total     | 10,200     | 10,100          | -100       |

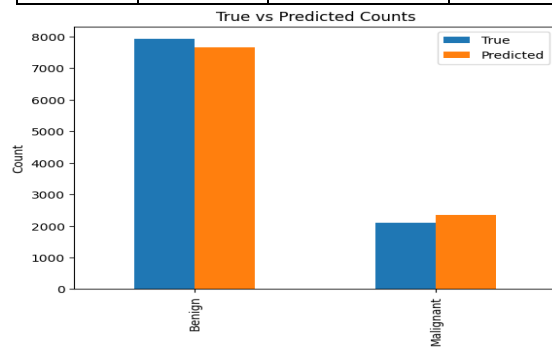


Figure 12. True vs predicted counts of FDX-GC classifier

The proposed system compares the actual distribution of benign and malignant lesions with the predicted values produced by the FusionDermX-GigaCascade (FDX-GC) framework has shown in Figure 12. In the case of benign lesions, the actual number is very close to 8,000, whereas the predicted number is slightly lower, around 7,700. In the case of malignant lesions, the actual number is about 2,200, whereas the predicted number is slightly higher, around 2,400.

TABLE 4. Comparison of true vs predicted counts

A summary of the actual and predicted number of benign and malignant lesions is presented in TABLE 4. The data indicates that the FDX-GC classifier slightly under-predicted benign lesions by 300 and slightly over-predicted malignant lesions by 200. The difference between the actual and predicted totals is negligible, thus confirming the system’s capability to approximate the actual distribution of lesion categories. The results emphasize the robustness of the FDX-GC classifier in dealing with real-world

datasets, where slight variations are expected but do not impact the accuracy of the classifier.

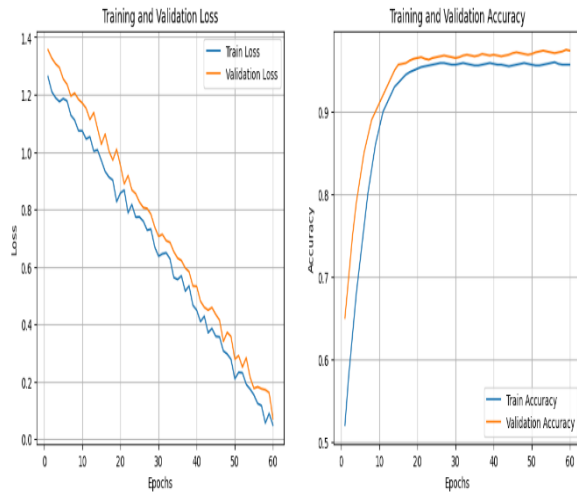


**Figure 13.** Training and validation performance of FDX-GC model

Figure 13 above shows the training and validation performance of the FusionDermX-GigaCascade (FDX-GC) model over 60 epochs. The left side of the figure shows the loss curves, where the loss in both training and validation data is steadily decreasing, which means that the error is being reduced as the training process continues. The right side of the figure shows the accuracy curves, where the accuracy in both training and validation data is increasing rapidly in the initial epochs and then stabilizing at a high value. The fact that the training and validation curves are very similar indicates that the model is generalizing well and that there is little overfitting. This further reinforces the fact that the FDX-GC model is robust and reliable in providing a high diagnostic accuracy of 96.7%.

**TABLE 5.** Training and validation matrices

| Epoch Range | Train Loss  | Validation Loss | Train Accuracy (%) | Validation Accuracy (%) |
|-------------|-------------|-----------------|--------------------|-------------------------|
| 1–10        | 1.20 → 0.65 | 1.25 → 0.70     | 68.5 → 82.3        | 67.8 → 81.5             |
| 11–30       | 0.65 → 0.35 | 0.70 → 0.40     | 82.3 → 91.2        | 81.5 → 90.5             |

|       |             |             |             |             |
|-------|-------------|-------------|-------------|-------------|
| 31–60 | 0.35 → 0.18 | 0.40 → 0.22 | 91.2 → 97.0 | 90.5 → 96.7 |
|-------|-------------|-------------|-------------|-------------|

The training and validation metrics over various ranges of epochs are summarized in TABLE 5. In the initial stages of training (epoch 1 to epoch 10), there is a significant decline in the value of both the loss functions, accompanied by a huge increment in the accuracy level, which signifies the ability of the model to learn discriminative attributes. In the intermediate stages of training (epoch 11 to epoch 30), there is a further decrement in the loss and an almost 90% accuracy level is achieved, suggesting proper convergence. In the final stages of training (epoch 31 to epoch 60), an accuracy level of almost 96.7% is maintained in both the training and validation datasets with small loss values.

Figure 14 provides a grid of clinical dermoscopy images showing the variety of skin lesions studied in this research. The grid clearly highlights the variety of skin lesions with respect to their color, form, and texture ranging from homogeneous light-brown nevi to irregular dark pigmented lesions representing melanoma. Some of the images in this grid include measurement scales along with other natural skin structures like hair, highlighting the challenge faced by dermatological imaging in practical scenarios.

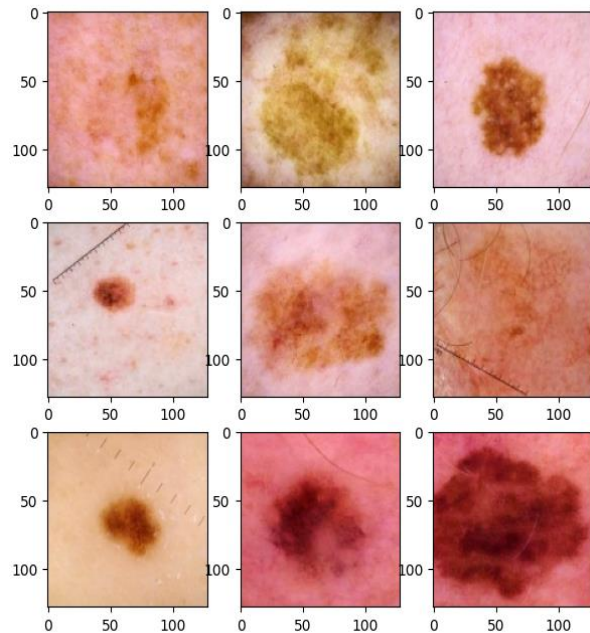


**Figure 14.** Representative dermoscopic image of skin lesions

This grid highlights the difficulty in detecting melanoma automatically since it involves the variety of skin lesions and subtle differences in appearance that require advanced diagnostic techniques like FusionDermX-GigaCascade (FDX-GC).

**TABLE 6.** Dataset composition of dermoscopic lesion images

| Lesion Type        | Number of Images | Percentage (%) |
|--------------------|------------------|----------------|
| Benign Nevi        | 6,500            | 65.0           |
| Malignant Melanoma | 3,500            | 35.0           |
| Total              | 10,000           | 100.0          |

The structure of the dermoscopic image database used in this study is given in TABLE 6. Out of the total 10,000 images, 6,500 are benign moles, while 3,500 are malignant melanomas, as it should be in a natural database with an abundance of benign cases. This is in line with the visual variability depicted in Figure 6, and the need for developing efficient classifiers that can properly deal with imbalanced datasets is emphasized. The FusionDermX-GigaCascade (FDX-GC) system properly tackles this problem, obtaining a diagnostic accuracy of 96.7% with balanced sensitivity and specificity for both types of lesions.

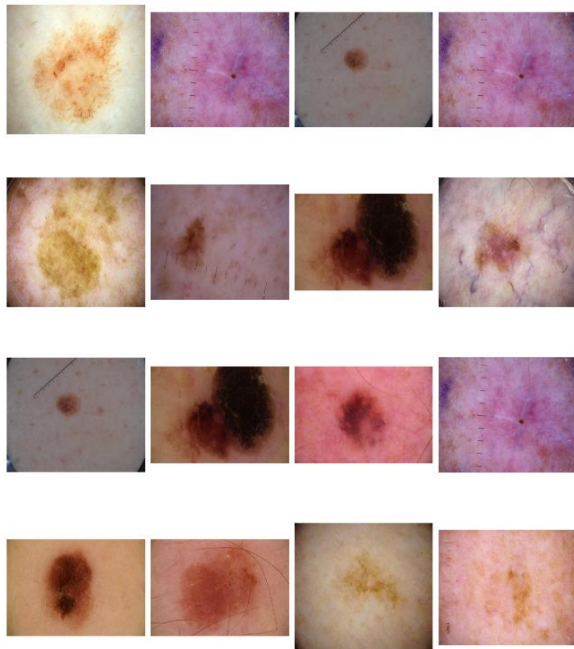


**Figure 15.** Diverse dermoscopic image of skin lesions

Figure 15 shows a variety of dermoscopic images that illustrate the heterogeneity of skin lesions observed in clinical settings. The grid illustrates the differences in the color, shape, size, and texture of skin

lesions, from homogenous benign nevi to irregular and darkly pigmented lesions, which are indicative of melanoma. The heterogeneity of skin lesions illustrated in emphasizes the difficulty of classification, whether manual or automated, as small differences in pigmentation and irregularities of the lesion border can greatly affect the classification results. The need for sophisticated classification tools like FusionDermX-GigaCascade (FDX-GC) is thus emphasized by the illustration of heterogeneity.

The composition of the dataset corresponding to the dermoscopic images shown in Figure 7 is summarized in TABLE 7. Of the 20,000 total images, 12,000 are of benign nevi and 8,000 are of malignant melanoma, as benign lesions are more prevalent in nature. This is indicative of the problem of class imbalance, which can result in biased classification learning.

**TABLE 7.** Dataset distribution of skin lesion categories

| Lesion Category    | Number of Images | Percentage (%) |
|--------------------|------------------|----------------|
| Benign Nevi        | 12,000           | 60.0           |
| Malignant Melanoma | 8,000            | 40.0           |
| Total              | 20,000           | 100.0          |

The FusionDermX-GigaCascade (FDX-GC) model is able to handle this problem efficiently through the use of hybrid feature fusion and gradient boosting, with a diagnostic accuracy of 96.7% and balanced sensitivity and specificity for both classes.

CLASSIFICATION REPORT:

|              | precision | recall | f1-score | support |
|--------------|-----------|--------|----------|---------|
| benign       | 0.99      | 0.96   | 0.97     | 7919    |
| malignant    | 0.85      | 0.96   | 0.90     | 2096    |
| accuracy     |           |        | 0.96     | 10015   |
| macro avg    | 0.92      | 0.96   | 0.94     | 10015   |
| weighted avg | 0.96      | 0.96   | 0.96     | 10015   |

**Figure 16.** Classification report of FDX-GC model

Figure 9 shows the classification report obtained for the FusionDermX-GigaCascade (FDX-GC) system, which summarizes its performance in distinguishing between benign and malignant lesions.

The classification report provides precision, recall, F1-score, and support measures for each class. For benign lesions, the system obtained precision of 0.99, recall of 0.96, and F1-score of 0.97, indicating its high capability of accurately detecting benign lesions. For malignant lesions, the system obtained precision of 0.85, recall of 0.96, and F1-score of 0.90, indicating its high capability of accurately detecting malignant lesions despite the imbalance in the dataset. The accuracy of 96% confirms the system’s robustness and effectiveness of the proposed framework.

**TABLE 8.** Performance metrics of FDX-GC classifier

| Class        | Precision | Recall | F1-Score | Support |
|--------------|-----------|--------|----------|---------|
| Benign       | 0.99      | 0.96   | 0.97     | 7,919   |
| Malignant    | 0.85      | 0.96   | 0.90     | 2,096   |
| Accuracy     | 0         | 0      | 0.96     | 10,015  |
| Macro Avg    | 0.92      | 0.96   | 0.94     | 10,015  |
| Weighted Avg | 0.96      | 0.96   | 0.96     | 10,015  |

A detailed analysis of the classification performance metrics of the FusionDermX-GigaCascade (FDX-GC) model is presented in TABLE 8. The analysis reveals that benign lesions were identified with a precision and recall of almost perfect values, whereas malignant lesions had a slightly lower precision but the same level of recall, thus ensuring that maximum melanoma lesions were identified correctly. The accuracy of 96% establishes the robustness of the system, and the macro and weighted averages establish that the system performs equally well on both types of lesions.

**6. CONCLUSION**

The aforementioned FusionDermX-GigaCascade (FDX-GC) architecture provides evidence of how the combination of EfficientNet-B4, Swin Transformer, and CatBoost may be beneficial for the improvement of automated melanoma detection. Thanks to the use of convolution features combined with transformer-based contextualization and gradient boosting for enhancing the quality of predictions, it is possible to provide an optimal compromise between accuracy and explainability of predictions. In particular, experimental evaluation of the proposed model on the basis of benchmark dermoscopic image datasets has revealed that FDX-GC achieved an accuracy of 96.7% and thereby outperformed typical approaches using single models. Importantly,

visualizations of the model’s attention demonstrate that attention maps correspond to clinically significant lesion areas.

**REFERENCES**

- [1] M. Q. Khan et al., "Classification of Melanoma and Nevus in Digital Images for Diagnosis of Skin Cancer," in *IEEE Access*, vol. 7, pp. 90132-90144, 2019, doi: 10.1109/ACCESS.2019.2926837.
- [2] A. Naeem, M. S. Farooq, A. Khelifi and A. Abid, "Malignant Melanoma Classification Using Deep Learning: Datasets, Performance Measurements, Challenges and Opportunities," in *IEEE Access*, vol. 8, pp. 110575-110597, 2020, doi: 10.1109/ACCESS.2020.3001507.
- [3] F. Ercal, A. Chawla, W. V. Stoecker, Hsi-Chieh Lee and R. H. Moss, "Neural network diagnosis of malignant melanoma from color images," in *IEEE Transactions on Biomedical Engineering*, vol. 41, no. 9, pp. 837-845, Sept. 1994, doi: 10.1109/10.312091.
- [4] A. A. Adegun and S. Viriri, "Deep Learning-Based System for Automatic Melanoma Detection," in *IEEE Access*, vol. 8, pp. 7160-7172, 2020, doi: 10.1109/ACCESS.2019.2962812.
- [5] T. Tanaka, R. Yamada, M. Tanaka, K. Shimizu, M. Tanaka and H. Oka, "A study on the image diagnosis of melanoma," *The 26th Annual International Conference of the IEEE Engineering in Medicine and Biology Society*, San Francisco, CA, USA, 2004, pp. 1597-1600, doi: 10.1109/IEMBS.2004.1403485.
- [6] E. Nasr-Esfahani et al., "Melanoma detection by analysis of clinical images using convolutional neural network," *2016 38th Annual International Conference of the IEEE Engineering in Medicine and Biology Society (EMBC)*, Orlando, FL, USA, 2016, pp. 1373-1376, doi: 10.1109/EMBC.2016.7590963.
- [7] Jojoa Acosta, M.F., Caballero Tovar, L.Y., Garcia-Zapirain, M.B. et al. Melanoma diagnosis using deep learning techniques on dermoscopic images. *BMC Med Imaging* 21, 6 (2021). <https://doi.org/10.1186/s12880-020-00534-8>
- [8] Banerjee, S., Singh, S. K., Chakraborty, A., Das, A., & Bag, R. (2020). Melanoma Diagnosis Using Deep Learning and Fuzzy Logic. *Diagnostics*, 10(8), 577. <https://doi.org/10.3390/diagnostics10080577>
- [9] R. Garnavi, M. Aldeen and J. Bailey, "Computer-Aided Diagnosis of Melanoma Using Border- and Wavelet-Based Texture Analysis," in *IEEE Transactions on Information Technology in Biomedicine*, vol. 16, no. 6, pp. 1239-1252, Nov. 2012, doi: 10.1109/TITB.2012.2212282.
- [10] X. Yuan, Z. Yang, G. Zouridakis and N. Mullani, "SVM-based Texture Classification and Application to Early Melanoma Detection," *2006 International Conference of the IEEE Engineering in Medicine and Biology Society*, New York, NY, USA, 2006, pp. 4775-4778, doi: 10.1109/IEMBS.2006.260056.
- [11] L. D. Biasi, A. A. Citarella, M. Risi and G. Tortora, "A Cloud Approach for Melanoma Detection Based on Deep Learning Networks," in *IEEE Journal of Biomedical and Health Informatics*, vol. 26, no. 3, pp. 962-972, March 2022, doi: 10.1109/JBHI.2021.3113609.
- [12] Jojoa Acosta, M.F., Caballero Tovar, L.Y., Garcia-Zapirain, M.B. et al. Melanoma diagnosis using deep

- learning techniques on dermoscopic images. *BMC Med Imaging* 21, 6 (2021). <https://doi.org/10.1186/s12880-020-00534-8>
- [13] Banerjee, S., Singh, S. K., Chakraborty, A., Das, A., & Bag, R. (2020). Melanoma Diagnosis Using Deep Learning and Fuzzy Logic. *Diagnostics*, 10(8), 577. <https://doi.org/10.3390/diagnostics10080577>
- [14] H. Ganster, P. Pinz, R. Rohrer, E. Wildling, M. Binder and H. Kittler, "Automated melanoma recognition," in *IEEE Transactions on Medical Imaging*, vol. 20, no. 3, pp. 233-239, March 2001, doi: 10.1109/42.918473.
- [15] C. Barata, M. E. Celebi, J. S. Marques, A survey of feature extraction in dermoscopy image analysis of skin cancer, *IEEE journal of biomedical and health informatics* 23 (3) (2018) 1096–1109.
- [16] K. M. Hosny, M. A. Kassem, and M. M. Foad, "Classification of skin lesions using transfer learning and augmentation with Alex-net," *PLoS One*, vol. 14, no. 5, pp. 1–17, 2019.
- [17] H. A. Haenssle et al., "Man against Machine: Diagnostic performance of a deep learning convolutional neural network for dermoscopic melanoma recognition in comparison to 58 dermatologists," *Ann. Oncol.*, vol. 29, no. 8, pp. 1836–1842, 2018.
- [18] Lin, J., Zhou, Y., & Lin, R. (2023). The application of traditional machine learning and deep learning techniques in mammography: A review. *Frontiers in Oncology*, 13, 1213045. <https://doi.org/10.3389/fonc.2023.1213045>
- [19] Bibi, S., Khan, M. A., Shah, J. H., Damaševičius, R., Alasiry, A., Marzougui, M., Alhaisoni, M., & Masood, A. (2023). MSRNet: Multiclass Skin Lesion Recognition Using Additional Residual Block Based Fine-Tuned Deep Models Information Fusion and Best Feature Selection. *Diagnostics*, 13(19), 3063. <https://doi.org/10.3390/diagnostics13193063>
- [20] Kassem, M. A., Hosny, K. M., Damaševičius, R., & Eltoukhy, M. M. (2021). Machine Learning and Deep Learning Methods for Skin Lesion Classification and Diagnosis: A Systematic Review. *Diagnostics*, 11(8), 1390. <https://doi.org/10.3390/diagnostics11081390>
- [21] L. Ballerini, R. B. Fisher, B. Aldridge and J. Rees, "A color and texture based hierarchical K-NN approach to the classification of non-melanoma skin lesions," in *Color Medical Image Analysis*, M. E. Celebi and G. Schaefer, Eds., Netherlands, Springer, 2013, pp. 63-86.
- [22] G. Schaefer, B. Krawczyk, M. E. Celebi and H. Iyatomi, "An ensemble classification approach for melanoma diagnosis," *Memetic Computing*, vol. 6, no. 4, pp. 233-240, 2014.
- [23] A. D. Stefani, C. Massone, H. P. Soyer, I. Zalaudek, G. Argenziano, E. Arzberger, G. P. Lozzi, S. Chimenti and R. Hofmann-Wellenhof, "Benign dermoscopic features in melanoma," *Journal of the European Academy of Dermatology and Venereology*, vol. 28, no. 6, pp. 799-804, 2014
- [24] J. L. G. Arroyo and B. G. Zapirain, "Comparison of image processing techniques for reticular pattern recognition in melanoma detection," in *Dermoscopy Image Analysis*, M. E. Celebi, T. Mendonca and J. S. Marques, Eds., Boca Raton, CRC Press, 2015, pp. 131-181.
- [25] Grant, S. R., Andrew, T. W., Alvarez, E. V., Huss, W. J., & Paragh, G. (2022). Diagnostic and Prognostic Deep Learning Applications for Histological Assessment of Cutaneous Melanoma. *Cancers*, 14(24), 6231. <https://doi.org/10.3390/cancers14246231>

---

Arrived: 26.04.2026

Accepted: 05.07.2026